

# NUMERICAL SIMULATION OF CAVITATING FLOWS CONSIDERING THE FLUID COMPRESSIBILITY IN OPENFOAM

CHANGCHANG WANG<sup>1</sup>, GUOYU WANG<sup>2</sup>, BIAO HUANG<sup>3</sup>

<sup>1</sup> School of Mechanical Engineering, Beijing Institute of Technology, Beijing, 100081, China, wangchangchang@bit.edu.com

<sup>2</sup> School of Mechanical Engineering, Beijing Institute of Technology, Beijing, 100081, China, wangguoyu@bit.edu.com

<sup>3</sup> School of Mechanical Engineering, Beijing Institute of Technology, Beijing, 100081, China, huangbiao@bit.edu.com

**Keywords:** Compressible cavitating flow, Tait equation of state, Shock wave emission, OpenFOAM

## Abstract

The objective of this paper is to address the simulation of transient cavitating flows with the compressibility of both water and vapour considered. The compressible phase volume fraction transport equations and compressible Pressure Possion equation with phase change are derived and a phase change algorithm is implemented into the native compressible two-phase flow solver compressibleInterFoam in OpenFOAM-4.0. The compressible governing equations together with the Tait equation of state for water and ideal gas equations of state for vapour are solved. The partial cavitating flow characterized by alternate effects of re-entrant flow and shock wave around a NACA66 hydrofoil is selected for the solver performance test. Comparisons are made between the results obtained by the native incompressible cavitation solver interPhaseChangeFoam and the present compressible cavitation solver. Results show that both the incompressible cavitation solver and compressible solver can predict the attached cavity growth, re-entrant flow development and large scale cloud cavity formation and shedding process, while the cloud cavity collapse induced shock wave phenomena which is highly related with the water/vapour compressibility is only captured by the implemented compressible cavitation solver. Moreover, the compressible cavitation solver can better predict cavitation evolution cycle and cavitation induced pressure fluctuations. The water compressibility is important for the wave dynamics in cavitating flows.

## Introduction

Cavitation occurs when pressure drops below vapour pressure in high speed liquid flows. Cavitation is the complex multiphase flow, consisting of mass transfer, multiphase, turbulence and compressibility. Experiments have identified the shock as one of main origins of cavitation instabilities except for the re-entrant flow, which will cause large scale pressure fluctuations, strong vibrations and noise. The wave dynamics in cavitating flows is highly associated with the fluid compressibility, requiring to solve the compressible cavitation governing equations, including continuity, momentum and energy equations. Thus the development of compressible cavitation solver has great significance. The purpose of this paper is to introduce an implementation of a compressible cavitation solver with transport equation cavitation in OpenFOAM and show its ability in capturing the cloud cavity collapse induced shock wave.

## Methods

In the present study, the compressible Navier-Stokes equations including continuity, momentum and energy equations, along with the transport equation for void fraction, are used as governing equations. To account for the fluid compressibility, the Tait equations of state for water and ideal gas equation of state for vapour are employed. The phase change algorithm is implemented into the native pressure-based compressible two-phase flow solver compressibleInterFoam. The compressible phase volume fraction transport equation and compressible Pressure Possion equation with phase change are derived.

The Tait equation of state for water

$$\frac{p_l+B}{p_{l,sat}+B} = \left( \frac{\rho_l}{\rho_{l,sat}} \right)^N \quad (1)$$

where  $p_{sat}=2338.6$  Pa and  $\rho_{sat}=998.16$  kg/m<sup>3</sup> are the saturation pressure and saturation density of liquid water at 293.15 K according to NIST data.  $B=3.06 \times 10^8$  Pa and  $N=7.1$  are the fitted constants.

The ideal gas equation of state for vapor

$$p_v = \rho_v R_v T_v \quad (2)$$

where subscript  $v$  denotes vapor-phase value and  $R_v=461.6$  J/(kg.K) is gas constant. In the present study, the non-condensable gas is ignored in the gas phase.

The Saito cavitation model and SST SAS turbulence model

$$\dot{m}^- = C_c \alpha^2 (1 - \alpha) \frac{\max((p - p_v), 0)}{\sqrt{2\pi R_g T}}, \text{ if } p > p_v \quad (3)$$

$$\dot{m}^+ = C_e \alpha^2 (1 - \alpha) \frac{\rho_l \max((p_v - p), 0)}{\rho_g \sqrt{2\pi R_g T}}, \text{ if } p < p_v \quad (4)$$

where  $\alpha$  is the void fraction,  $\rho_l$  is the liquid density,  $\rho_v$  is the vapor density,  $R_g$  is the gas constant,  $T$  is the local fluid temperature,  $p_v$  is the saturated liquid vapor pressure and  $p$  is the local fluid pressure.  $C_c$  is the rate coefficient for reconversion of vapor back into liquid when local pressure exceeds the saturated vapor pressure.  $C_e$  is the rate coefficient for vapor generated from liquid when local pressure below the saturated vapor pressure. In the present study,  $C_c = C_e = 0.1$  is taken. The von Karman length-scale and the SAS term are as following

$$L_{vK} = \kappa \left| \frac{\partial U / \partial y}{\partial^2 U / \partial y^2} \right| \quad (5)$$

$$Q_{SAS} = \max \left[ \rho \zeta_2 S^2 \left( \frac{L}{L_{vK}} \right)^2 - C_{SAS} \frac{2\rho k}{\sigma_\Phi} \max \left( \frac{1}{k^2} \frac{\partial k}{\partial x_j} \frac{\partial k}{\partial x_j}, \frac{1}{\omega^2} \frac{\partial \omega}{\partial x_j} \frac{\partial \omega}{\partial x_j} \right), 0 \right] \quad (6)$$

Where  $\zeta_2 = 3.51$ ,  $\sigma_\Phi = 2/3$ ,  $C_{SAS} = 2.0$ ,  $L = \sqrt{k} (c_\mu^{1/4} \cdot \omega)$  is the length scale of the modeled turbulence.

The compressible phase volume fraction transport equation with phase change is derived as following:

$$\frac{\partial \alpha_1 \rho_1}{\partial t} + \nabla \cdot (\rho_1 \alpha_1 U) = \dot{m} \quad (7)$$

$$\frac{\partial \alpha_2 \rho_2}{\partial t} + \nabla \cdot (\rho_2 \alpha_2 U) = -\dot{m} \quad (8)$$

Expanding the Eq. (7), then:

$$\frac{\partial \alpha_1}{\partial t} + \nabla \cdot (\alpha_1 U) = -\frac{\alpha_1}{\rho_1} \frac{D\rho_1}{Dt} + \frac{\dot{m}}{\rho_1} \quad (9)$$

The similar as Eq. (8):

$$\frac{\partial \alpha_2}{\partial t} + \nabla \cdot (\alpha_2 U) = -\frac{\alpha_2}{\rho_2} \frac{D\rho_2}{Dt} + \frac{\dot{m}}{\rho_2} \quad (10)$$

Add Eq. (9) and Eq. (10), then,

$$\nabla \cdot U = -\left( \frac{\alpha_1}{\rho_1} \frac{D\rho_1}{Dt} + \frac{\alpha_2}{\rho_2} \frac{D\rho_2}{Dt} \right) + \dot{m} \left( \frac{1}{\rho_1} - \frac{1}{\rho_2} \right) \quad (11)$$

Expanding Eq. (9), then

$$\frac{\partial \alpha_1}{\partial t} + \alpha_1 \nabla \cdot U + U \nabla \alpha_1 = -\frac{\alpha_1}{\rho_1} \frac{D\rho_1}{Dt} + \frac{\dot{m}}{\rho_1} \quad (12)$$

Substituting Eq. (11) into Eq. (12)

$$\frac{\partial \alpha_1}{\partial t} + \nabla \cdot (\alpha_1 U) = \alpha_1 \alpha_2 \left( \frac{1}{\rho_2} \frac{D\rho_2}{Dt} - \frac{1}{\rho_1} \frac{D\rho_1}{Dt} \right) + \dot{m} \left[ \frac{1}{\rho_1} - \alpha_1 \left( \frac{1}{\rho_1} - \frac{1}{\rho_2} \right) \right] + \alpha_1 \nabla \cdot U \quad (13)$$

The interface compression term is implemented, thus

$$\frac{\partial \alpha_1}{\partial t} + \nabla \cdot (\alpha_1 U) + \nabla \cdot (U_r \alpha_1 \alpha_2) = \alpha_1 \alpha_2 \left( \frac{1}{\rho_2} \frac{D\rho_2}{Dt} - \frac{1}{\rho_1} \frac{D\rho_1}{Dt} \right) + \dot{m} \left[ \frac{1}{\rho_1} - \alpha_1 \left( \frac{1}{\rho_1} - \frac{1}{\rho_2} \right) \right] + \alpha_1 \nabla \cdot U \quad (14)$$

Where  $U_r$  is the modelled relative velocity, defined as

$$U_r = c_\alpha |U| \quad (14)$$

Where  $c_\alpha$  is a parameter used to adjust the strength of the compression of interface. The equation is solved explicitly with the MULES (multidimensional universal limiter with explicit solution) scheme in several sub-cycle within a time step.

The compressible Pressure Possion equation is derived as follows:

Thermodynamics equation of state:

$$\rho = \Psi p \quad (15)$$

Where  $\Psi$  is the compressible coefficient. Substitute Eq. (15) into Eq. (7), then

$$\frac{\partial (\Psi_1 \alpha_1 p)}{\partial t} + \nabla \cdot (\Psi_1 \alpha_1 p U) = \Psi_1 \frac{\partial \alpha_1 p}{\partial t} + \alpha_1 p \frac{\partial \Psi_1}{\partial t} + \Psi_1 \alpha_1 p \nabla U + U \nabla (\Psi_1 \alpha_1 p) = \dot{m} \quad (16)$$

Expand Eq. (16), then

$$\Psi_1 \frac{D\alpha_1 p}{Dt} + \rho_1 \nabla U = \dot{m} \quad (17)$$

Similarly, Eq. (8) can be rearranged as

$$\Psi_2 \frac{D\alpha_2 p}{Dt} + \rho_2 \nabla U = -\dot{m} \quad (18)$$

Finally, the compressible Pressure Possion equation with phase change is as following

$$\left( \frac{\alpha_1}{\rho_1} \Psi_1 + \frac{\alpha_2}{\rho_2} \Psi_2 \right) \left( \frac{\partial p}{\partial t} + U \nabla \cdot p \right) + \nabla \cdot U = \left( \frac{\alpha_1}{\rho_1} - \frac{\alpha_2}{\rho_2} \right) \dot{m} \quad (19)$$

## Results

The numerical results are shown for both the present compressible cavitation solver and the native incompressible cavitation solver `interPhaseChangeFoam`. Fig. 1 shows the time evolution of cavity volume obtained by both the compressible and incompressible results. The comparisons of the experimentally measured and numerically predicted cavitation evolution frequency based on the cavity volume evolution are shown in Tab. 1, in which the relative error is also presented. The Saito cavitation model and the SST SAS turbulence model are used for both incompressible and compressible simulation. It can be observed that the cavity volume predicted by the present compressible solver is

larger than that the incompressible solver. The cavity evolution frequency in Tab. 1 indicates that the present compressible cavitating flow solver could predict the unsteady cavitation frequency more precisely.

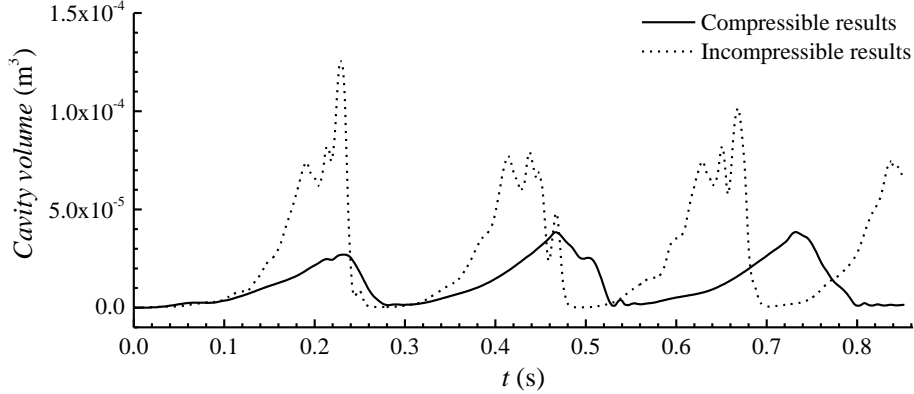


Figure 1: Comparisons of the time evolution of cavity volume based on compressible solution and incompressible solution.

Table 1: Comparisons of the measured (Exp., Leroux et al., 2014) and numerically predicted (Num.) cavity evolution frequency.

	Exp. [4]	Num. (Incompressible)	Num. (Compressible)
Mean value $f$ (Hz)	3.625	4.504 (24.2 %)	3.867 (6.7 %)

The comparisons of the absolute pressure evolution between the compressible results, incompressible results and the experiments data at  $x/c=0.7$  during 0.64 s are shown in Fig. 2. It can be found that the numerically predicted absolute pressure magnitude agrees well with the experiment data. However, the cavity cloud collapse induced shock wave is only captured by the compressible results. The pressure evolution frequency agrees with the cavity behaviours evolution.

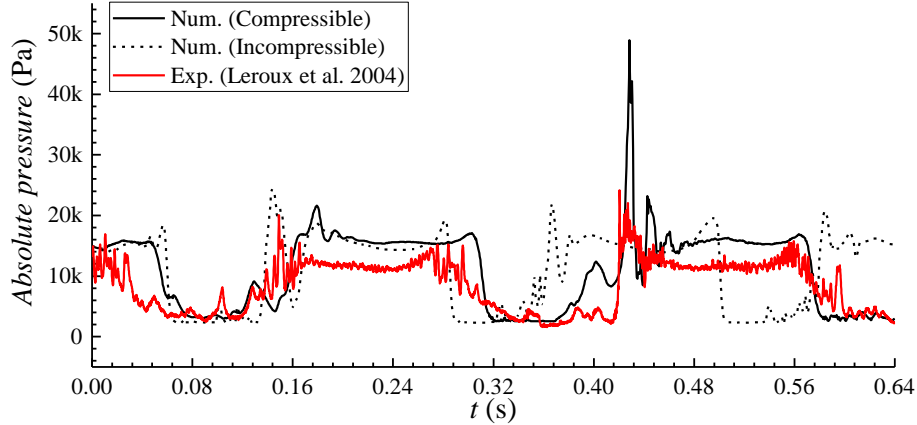


Figure 2: Comparisons of the absolute pressure evolution predicted by the compressible solver with the experiments data and incompressible solver results at  $x/c=0.7$ .

## Conclusions

In this paper, a compressible cavitation solver is developed by implementing the phase change algorithm into the native compressible two-phase flow solver compressibleInterFoam in OpenFOAM-4.0, considering the compressibility of both water and vapour. The thermodynamic equations of state with Tait state equation for water and ideal gas state equation for vapour are employed. The Saito cavitation model and the SST-SAS turbulence model are applied to simulate the turbulent cavitating flow. The cloud cavity collapse induced shock wave dynamics and its interaction with the attached cavity sheet growth is well predicted by the implemented compressible cavitation solver. The attached cavity sheet growth, the re-entrant flow development and the large scale cloud cavity shedding can be simulated well by both the incompressible cavitation solver, while the cavitation dynamics associated with the compressibility, such as the shock wave dynamics, can only be predicted by the compressible cavitation solver, which considers the compressibility of both water and vapour.

## Acknowledgements

The authors gratefully acknowledge support by the National Foundation of China (NSFC, Grant No: 91752105), National Natural Science Foundation of Beijing (Grant No: 3172029), the Open Foundation of State Key Laboratory of Ocean Engineering (Shanghai Jiao Tong University, China), and Graduate Technological Innovation Project of Beijing Institute of Technology (Grant No: 2017CX10017).

## References

- [1] R. Issa, A. Gosman, A. Watkins, The computation of compressible and incompressible recirculating flows by a non-iterative implicit scheme, *J. Comput. Phys.* 62 (1986): 66-82.

- [2] H. Jasak, Error analysis and estimation for the definite volume method with applications to fluid flows. University of London: 1996. Ph.D. Thesis.
- [3] S. Miller, H. Jasak, D. Boger, F. Paterson and A. Nedungadi, A pressure-based, compressible, two-phase flow finite volume method for underwater explosions, *Comput. Fluids* 38 (2013) 132-143.
- [4] J.B. Leroux, J.A. Astolfi and J.Y. Billard, An experimental study of unsteady partial cavitation, *J. Fluids. Eng.* 126 (2004) 94-101.